

Dielectric and electro-optic studies of a bimesogenic liquid crystal composed of bent-core and calamitic units

R. Balachandran,¹ V. P. Panov,^{1,2} J. K. Vij,^{1,*} G. Shanker,^{3,4} C. Tschierske,³ K. Merkel,⁵ and A. Kocot⁶

¹*Department of Electronic and Electrical Engineering, Trinity College Dublin, The University of Dublin, Dublin 2, Ireland*

²*School of Physics and Astronomy, University of Manchester, M13 9PL Manchester, United Kingdom*

³*Institute of Chemistry, Organic Chemistry, Martin-Luther-University Halle-Wittenberg, Kurt-Mothes-Strasse 2, 06120 Halle, Germany*

⁴*BMS R&D Centre, BMS College of Engineering, Bull Temple Road, Bangalore-560019, India*

⁵*Central Mining Institute, Katowice, Poland*

⁶*Institute of Physics, Silesian University, Katowice, Poland*

(Received 3 June 2014; revised manuscript received 2 August 2014; published 29 September 2014)

A bimesogen, BR1, composed of a bent-core and calamitic unit, linked laterally via a flexible spacer is investigated by dielectric and electro-optic techniques. X-ray results show the presence of clusters in the nematic phase, and the cluster size is of the order of the thickness of a single layer. The splitting of the small-angle scattering $\Delta\chi/2$ is about 50° , which indicates SmC like clusters with a significant tilt of the molecules in the quasilayers. The sign reversal of the dielectric anisotropy $\Delta\epsilon'$ is observed as a function of frequency; the behavior is rather similar to that exhibited by the conventional dual frequency nematics, composed of a calamitic mesogen, with the exception that it occurs at much lower frequencies in this material. Interestingly, as the bimesogen enters its nematic phase, the average permittivity decreases as the temperature is lowered. This indicates the onset of antiparallel association of some of the dipoles in the system, and this type of association is much more prominent in BR1 in comparison to other bent-core liquid crystalline systems composed of the same bisbenzoate core unit. The analysis of the dielectric spectra using the Maier-Meier model confirms the onset of an antiparallel correlation of dipoles occurring at the isotropic to nematic phase transition temperature. Additionally these results support a model of the cluster where the transverse dipole moments in the neighboring layers are antiparalleled to each other.

DOI: [10.1103/PhysRevE.90.032506](https://doi.org/10.1103/PhysRevE.90.032506)

PACS number(s): 42.70.Df, 61.30.Eb, 77.22.Ch

I. INTRODUCTION

The molecular structure of a liquid crystalline (LC) material is found to significantly influence its properties and phase behavior. LC bimesogens, composed of two mesogenic units connected by a flexible spacer are of profound interest due to a range of the interesting phenomena exhibited by them. Some of these properties are often different from those of the constituent single mesogens [1]. These bimesogens also referred to as dimers can be symmetric or asymmetric and are classified into those consisting of (a) identical mesogenic units or (b) combining different types of units: such as the two nonidentical rodlike (RL) molecules [2] or bent-core (BC) molecules [3] or a calamitic unit connected to a bent core [4] or a discotic [5]. These mesogens are linked together by a flexible spacer (usually alkyl or alkoxy) [6]. The material properties in the resulting compounds are not only influenced by the constituent mesogens, but also influenced by the parity of the spacer that connects the two monomers [2]. For example, bimesogens with an even parity spacer is known to have linear conformations; the material properties in such bimesogens are similar to those of the individual rodlike molecules. The bimesogens with an odd parity spacer have an overall bent shape, and some of their properties are similar to those of the bent-core materials [2]. Furthermore, a combination of mesogenic units differing in shape [7], polarity, or compatibility [2,8] of the constituent units has resulted in compounds displaying a wide range of interesting properties—often distinct from those exhibited by the individual mesogens.

On connecting the two bent-core mesogens or calamitic units with a flexible spacer, the molecular system leads to many novel and complex phase sequences. For example, the twist-bend nematic (N_{tb}) phase observed in bimesogens composed of two rodlike molecules connected by an odd spacer has recently attracted considerable attention owing to a number of novel properties [9] exhibited by this phase including the appearance of spontaneous stripes of a well defined periodicity observed parallel to the rubbing direction in planar aligned cells. Such novel properties are usually absent in the ordinary nematic phase of these compounds. Dantlgraber *et al.* [3(a)] reported the first example of a bimesogen combining the two bent-core molecules linked by dimethylsiloxane units. Several ferroelectric and antiferroelectric polar SmC phases were observed in some of these compounds depending on the spacer length. It is also possible to combine a bent-core and a rodlike mesogen to form a dimesogen. A number of studies have been performed on the terminal combinations of such dimesogens [4], and these are reported to have unusual liquid crystalline properties by Tamba *et al.* [4(a)]. The mesophasic behavior was found to be strongly dependent on the size and the structure of the calamitic unit and on the length and the parity of the spacer.

There has been a continued interest in the dielectric studies of the nematic phase of bimesogens as the dielectric properties are sensitive to both the dipole moment and the ordering of molecules. The interaction between the bulk liquid crystal and the electric field depends on the dielectric permittivity parallel (ϵ'_{\parallel}) and perpendicular (ϵ'_{\perp}) to the LC director and the difference between these two quantities ($\Delta\epsilon'$). The dielectric anisotropy $\Delta\epsilon'(\epsilon'_{\parallel} - \epsilon'_{\perp})$ is one of the important parameters of a LC material used in designing LC based devices and plays

*Corresponding author: jvij@tcd.ie

an important role in determining the effect of an electric field on such systems. Depending on the sign of $\Delta\epsilon'$ and the cell configuration, the director can be realigned by the electric field. The reorientation of the director via *Fréedericksz* transition causes the optical properties of the sample to change—the phenomenon exploited in many commercial LC applications. The sign of $\Delta\epsilon'$ can be positive or negative and may change from one to the other at some frequency as is observed in many calamitics [10] and BC systems [11,12]. Such nematics are labeled as dual frequency nematic (DFN) LCs. In the conventional DFNs, $\Delta\epsilon'$ is positive at lower frequencies and negative at higher frequencies, and the frequency at which the sign reversal occurs is called the crossover frequency f_c . Since the sign reversal of $\Delta\epsilon'$ provides a vast improvement in the switching ON and OFF response times of these nematics to the conventional ones [13], the dual frequency nematics are of particular interest in device applications. Faster ON and OFF switching is simply achieved by varying the frequency of the driving signal. In most calamitics the frequency at which the sign reversal of $\Delta\epsilon'$ occurs is too high for applications, whereas in BC nematics (BCNs) [11,12] this occurs at lower frequencies of technological interest.

In this paper, we investigate the dielectric and electro-optic properties of a bimesogen or sometimes called dimesogen, BR1 [14], composed of a bent-core and a calamitic mesogen. The two units are linked laterally via a flexible spacer [14]. Although various studies have been performed on dimesogens composed of rodlike and bent-core mesogens connected by terminal spacers, here we perform a study on the laterally connected dimesogens. We observe that the material exhibits a low frequency relaxation mode and the sign of $\Delta\epsilon'$ changes with frequency; the crossover frequency is found to be much lower than that of conventional nematics or the systems known so far.

II. EXPERIMENTAL METHOD

The synthesis and x-ray results of BR1 are reported in Ref. [14]. BR1 is composed of bent-core unit and calamitic mesogens, and these two are linked laterally by a flexible spacer. The molecular structure and the phase transition temperatures are given in Fig. 1(a); Fig. 1(b) shows the set-up for the alignment of the director by the magnetic field. The material exhibits a nematic phase on cooling from the isotropic phase. X-ray diffraction (XRD) results reveal that SmC type clusters are present in the nematic phase of this material with the cluster size being on the order of the thickness of a single layer. Furthermore, splitting of the small-angle scattering $\Delta\chi/2$ is $\sim 50^\circ$ indicating a significant tilt of the molecules in these SmC like clusters [14].

In this paper, the material properties of the bimesogen are investigated through dielectric and electro-optic spectroscopies. Sandwich liquid crystal cells were prepared by using two indium tin oxide (ITO) glass plates with a sheet resistance of $20 \Omega/\square$. The sheet resistance was chosen to be as low as possible, such as to shift the peak frequency >1 MHz. The peak frequency in the dielectric spectrum is caused by the ITO layer in series with the cell capacitance. The glass substrates were spin coated with polymer aligning agents RN1175 (Nissan Chemicals, Japan) and AL60702 (JSR, Korea) and were cured at appropriate temperatures to

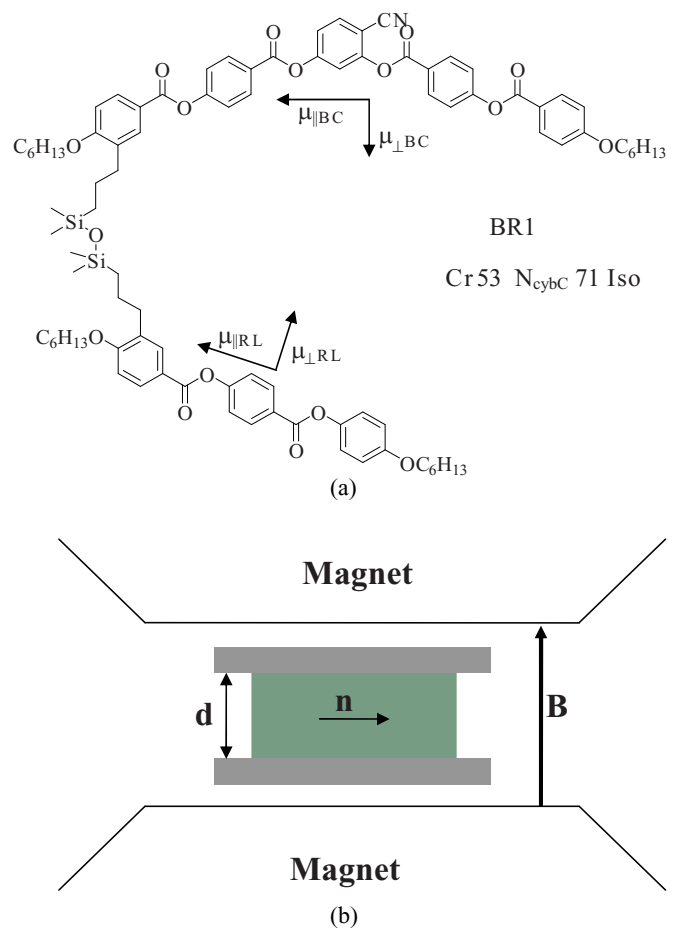


FIG. 1. (Color online) (a) Chemical structure and the transition temperatures of the dimesogenic material under study Iso = isotropic, N_{cybc} = cybotactic nematic phase composed of SmC clusters, Cr = Crystalline [14]. Electric dipole components determined by molecular modeling for individual mesogens were estimated to be as follows: $\mu_{\parallel BC} = 3.12$ D, $\mu_{\perp BC} = 5.18$ D, $\mu_{\parallel RL} = 2.45$ D, and $\mu_{\perp RL} = 2.96$ D. (b) shows the sample geometry used in the measurements of the parallel component of permittivity, obtained by inducing a homeotropic alignment on application of a magnetic field (**B**) in a direction perpendicular to the director (**n**) of the originally planar aligned cell.

obtain planar and homeotropic alignments, respectively, of the sample. The cells for the homogeneous alignment were rubbed and were assembled in such a way that the rubbing directions on the top and bottom substrates were antiparallel. The cell thickness was determined by using a spectrometer (Avaspec-2048) interfaced with a PC. The typical thickness used in the experiment was $\sim 26.2 \mu\text{m}$. The empty capacitance of the cell was measured before filling it with the material. The sample was then capillary filled by heating the empty cell well into the isotropic phase of the sample using a temperature controller (Eurotherm 2604). The setup consisting of a polarizing optical microscope (Leitz Laborlux 12 POL S) and a signal generator (Agilent 33120 A) was used to obtain the optical textures and to study the electro-optic behavior. The perpendicular component of the dielectric permittivity was obtained from dielectric measurements on a planar cell

using a Novocontrol Alpha high resolution dielectric analyzer (Novocontrol GmbH, Germany). The parallel component was obtained by placing the planar cell, mounted on a hot stage, between the poles of a large electromagnet, and by applying a field of 1 T perpendicular to the director orientation. The dielectric permittivity was measured in the frequency range of 1 Hz to 10 MHz as the sample was slowly cooled from the isotropic state. Normally in dielectric spectroscopy, we apply a weak field so as to study the material in the linear field induced regime and determine the dominant effects [15].

III. RESULTS AND DISCUSSIONS

Preliminary investigations in the planar and homeotropic cells showed that the material aligns reasonably well in a homogeneously planar cell; however it does not align homeotropically using the alignment agent alone. Although it was readily possible to obtain the perpendicular component using a planar cell, the parallel component was determined by placing the homogeneously aligned cell in a temperature regulated oven and by mounting the cell holder between the two poles of an electromagnet [Fig. 1(b)]. A magnetic field (\mathbf{B}) of strength 1 T was applied to orient the director \mathbf{n} along the magnetic field. The cell thickness was optimized until a reasonable homeotropic alignment was achieved. Since the critical field for the onset of the director deformations B_{th} is inversely related to the cell thickness d , a larger d implies a smaller threshold field for the *Fréedericksz* transition. This enables a complete switching of the cell to a homeotropic state for the maximum magnetic field applied across the cell.

Figure 2 compares the dielectric anisotropy as a function of the reduced temperature ($T - T_{NI}$), where T_{NI} is the nematic-isotropic (NI) transition temperature, obtained by subtracting the permittivity values obtained for the induced homeotropic (ϵ'_{\parallel}) alignment and the originally planar (ϵ'_{\perp}) cell for three different cell thicknesses (5, 12.7, and 26.2 μm) at a frequency of 6 kHz. It can be seen that for a 5 μm cell, a magnetic field of 1 T is not sufficient to switch it to a homeotropic state. As the cell thickness is increased, significant changes can be seen in the results given in Fig. 2 where there is a large difference in $\Delta\epsilon'$ between the 5 and the 12.7 μm cells, whereas this difference is greatly reduced between the 12.7 and the 26.2 μm cells. For cell thicknesses greater than 26.2 μm , this difference in $\Delta\epsilon'$ is expected to be even smaller. Hence, it can be safely assumed that for a cell of thickness 26.2 μm , a field of 1 T is reasonably large enough to align the material homeotropically.

The temperature dependence of the real part of dielectric permittivities ϵ'_{\perp} and ϵ'_{\parallel} and the average permittivity $\langle\epsilon'\rangle$ is shown in Fig. 3 for preselected frequencies of 100 Hz and 6 kHz. The parallel (ϵ'_{\parallel}) and perpendicular (ϵ'_{\perp}) permittivities were obtained from homeotropic and planar configurations of a 26.2 μm cell. Figure 3 clearly shows that the sign of $\Delta\epsilon'$ is positive at lower frequencies and turns negative at higher frequencies. The most interesting aspect being that the average permittivity $\langle\epsilon'\rangle$ decreases with a reduction in temperature, which in the ideal case should be similar to the values extrapolated from that in the isotropic phase. This suggests an onset of antipolar association of the dipoles at the isotropic to nematic transition temperature.

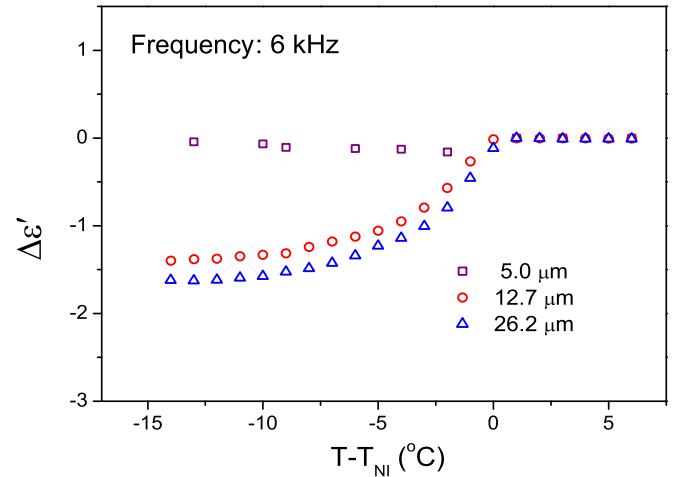


FIG. 2. (Color online) The dielectric anisotropy measured at a frequency 6 kHz is compared for cells with different cell thicknesses (~ 5 , 12.7, and 26.2 μm). The changes in $\Delta\epsilon'$ are higher as the cell thickness is increased. Although the dielectric permittivity between the planar and the apparent homeotropic states in the 5 μm cell is close to each other (indicating that the cell has not really switched to a homeotropic state), the change is much more noticeable in cells of 12.7 and 26.2 μm thicknesses. The difference in $\Delta\epsilon'$ between the 12.7 and the 26.2 μm cells is not as large as between 5.0 and 12.7 μm , and hence it can be safely assumed that the molecular alignment in the thicker cell of 26.2 μm has reasonably switched to a homeotropic state.

The sign reversal of the dielectric anisotropy was also confirmed using the optical contrast spectroscopy. This electro-optic method is based on the reorientation of the director under an applied field caused by the *Fréedericksz* transition, which in turn changes the optical properties of the sample. The setup for optical contrast spectroscopy consists of a Leitz polarizing microscope, photodiode, and a National Instruments data acquisition board interfaced to a PC. Measurements were carried out on a 5 μm planar cell as the material is cooled from

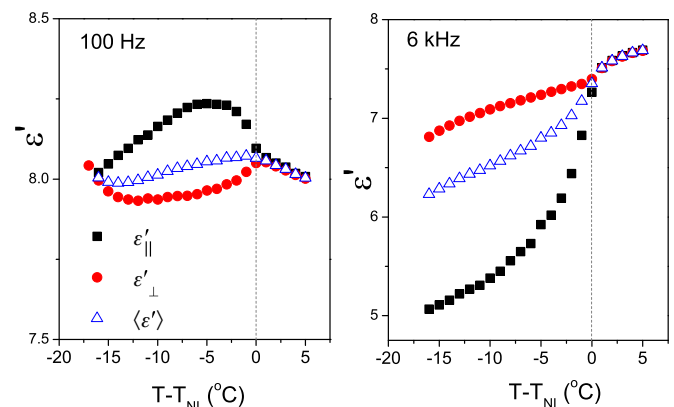


FIG. 3. (Color online) The real part of dielectric permittivity plotted as a function of reduced temperatures for frequencies 100 Hz and 6 kHz. The values of (ϵ'_{\parallel}) and (ϵ'_{\perp}) are obtained from the homeotropic and planar cell configurations, respectively, for a cell of thickness 26 μm . The average permittivity is defined as $\langle\epsilon'\rangle = \frac{1}{3}(\epsilon'_{\parallel} + 2\epsilon'_{\perp})$.

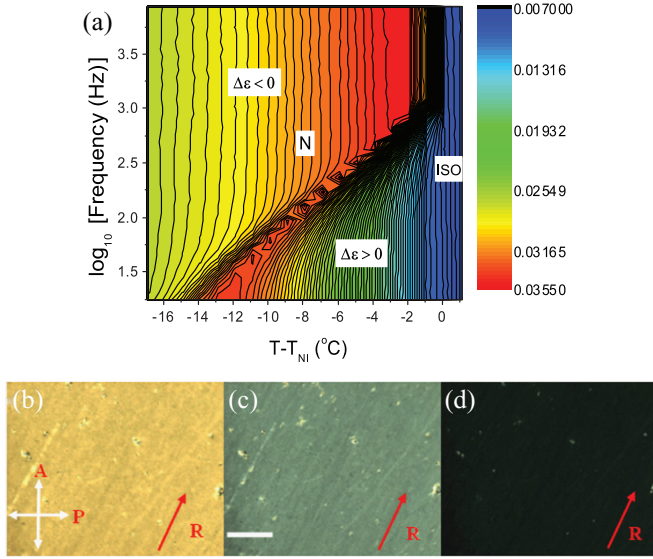


FIG. 4. (Color online) (a) Frequency-temperature plots of the transmittance curve obtained in a $5 \mu\text{m}$ planar cell under an applied field of $2 \text{ V}/\mu\text{m}$. The contour line implies a constant value of transmittance. (b)–(d) Textures obtained between crossed polarizers for $T/T_{\text{NI}} = 0.93$; R (red arrow) in each of the figures denotes the rubbing direction, and this is set at angle $\sim 22.5^\circ$ from the polarizer axis. (b) No field applied; (b) 6 V_{pk} , 50 Hz and (c) 15 V_{pk} , 50 Hz , the cell switches to an almost homeotropic state. The length of the white bar in (c) is $60 \mu\text{m}$. All pictures were taken with a fixed exposure time of 130 ms .

the isotropic to the nematic phase under an electric field of $\sim 2 \text{ V}/\mu\text{m}$ applied across the cell. Through this technique [11] the sign of $\Delta\epsilon'$ is optically determined for very low frequencies since this method is insensitive to the dc conductivity. The

latter is known to easily corrupt the dielectric results at lower frequencies.

Figure 4(a) presents the transmittance as a function of temperature and frequency (plotted on the \log_{10} scale) using the optical spectroscopy technique [11] where an electric field of $2 \text{ V}/\mu\text{m}$ of different frequencies is applied across the cell. In Fig. 4(a), the lines represent constant transmittance values, whereas the colors depict arbitrary levels of transmittance. The crowded lines are related to a rapid change in the transmittance due to *Fréedericksz* transition. For a reduced temperature of $T - T_{\text{NI}} = -5^\circ \text{C}$ the material shows positive $\Delta\epsilon'$ for frequencies $< 300 \text{ Hz}$, and it turns negative for frequencies greater than 300 Hz . As seen from Fig. 4(a), the sign reversal of $\Delta\epsilon'$ is observed as a function of frequency; however there is no specific temperature for which the sign reversal occurs as opposed to what was observed for a bent-core material composed of the same bisbenzoate core in the nematic phase [11(a)]. Such behavior nevertheless is similar to that observed in conventional DFNs composed of calamitic molecules with the exception that the sign reversal occurs at much lower frequencies in this material.

Figures 4(b)–4(d) show the textures obtained for the material using polarizing optical microscopy. *Fréedericksz* transition effects were observed at lower frequencies ($\ll 1 \text{ kHz}$); for example, see Figs. 4(c) and 4(d) for a frequency of 50 Hz . However no electrohydrodynamic patterns were observed for a maximum applied field of $5 \text{ V}/\mu\text{m}$ and frequencies up to 20 Hz . This confirms that a change in the transmittance spectra observed in Fig. 4(a) is due to *Fréedericksz* transition alone. In order to perform better analysis of the various dielectric modes of the system, the derivative of the real part of the permittivity with respect to $\ln f$, $d\epsilon'/d(\ln f)$ [16] for both sets of data are analyzed [Figs. 5(a) and 5(b)] using the equations,

$$\frac{d\epsilon'}{d(\ln f)} = \frac{d\epsilon'}{d(\ln \omega)} = \sum_{j=1}^n \text{Re} \frac{\delta\epsilon_j \alpha (i\omega\tau_j)^\alpha}{[1 + (i\omega\tau_j)^\alpha]^2}, \quad (1)$$

$$\frac{d\epsilon'}{d(\ln \omega)} = \sum_{j=1}^n \frac{\delta\epsilon_j \alpha_j (\omega\tau_j)^{\alpha_j} \{2(\omega\tau_j)^{\alpha_j} + [1 + (\omega\tau_j)^{2\alpha_j} \cos \frac{\pi\alpha_j}{2}] \cos \frac{\pi\alpha_j}{2}\}}{[1 + (\omega\tau_j)^{2\alpha_j} + 2(\omega\tau_j)^{2\alpha_j} \cos \frac{\pi\alpha_j}{2}]^2}. \quad (2)$$

Here, j is the variable denoting the number of relaxation processes up to n , τ_j is the relaxation time of the j th process (related to the relaxation frequency f_j or angular frequency ω_j as $\tau_j = 1/\omega_j = 1/2\pi f_j$), α is the fitting parameter, and $\delta\epsilon_j$ is the dielectric relaxation strength of the j th process. The dielectric strength ($\delta\epsilon_j$) for each process is determined from the fitting of the data to the above equation.

We find that the derivative method for the analysis of the dielectric modes is more convenient and has a better resolution of peaks than using the dielectric loss spectrum alone. Moreover, the dielectric loss data include dc conductivity, whose effect is rather dominant at lower frequencies and consequently making the spectra difficult to deconvolute [16]. The peak positions resolved using the derivative technique coincide with that for ϵ'' as demonstrated in Figs. 5(a) and 5(b). The spectra of $(d\epsilon'/d \ln f)$ shown in Fig. 5(a) reveal at

least three relaxation peaks for the planar configuration. These are P1, P2, and P3, plus the highest frequency peak P_{ITO} , which is due to the ITO resistance in series with the cell capacitance. Similarly for homeotropic alignment, three peaks H1, H2, and H_{ITO} are clearly seen in Fig. 5(b). An additional peak, H0 (not shown), appears below peak H1 at lower frequencies ($f < 10 \text{ Hz}$). However, this can only be resolved closer to the isotropic to nematic transition temperature.

The dielectric strength $\delta\epsilon$ obtained for the various processes is plotted as a function of reduced temperature in Fig. 6. The temperature dependence of the relaxation frequency for different processes is presented by the Arrhenius plot in Fig. 7 where the relaxation frequency f_R is plotted versus the inverse of the absolute temperature $1/T$.

In liquid crystals composed of calamitic mesogens, the frequency dependent dielectric permittivity can be analyzed in

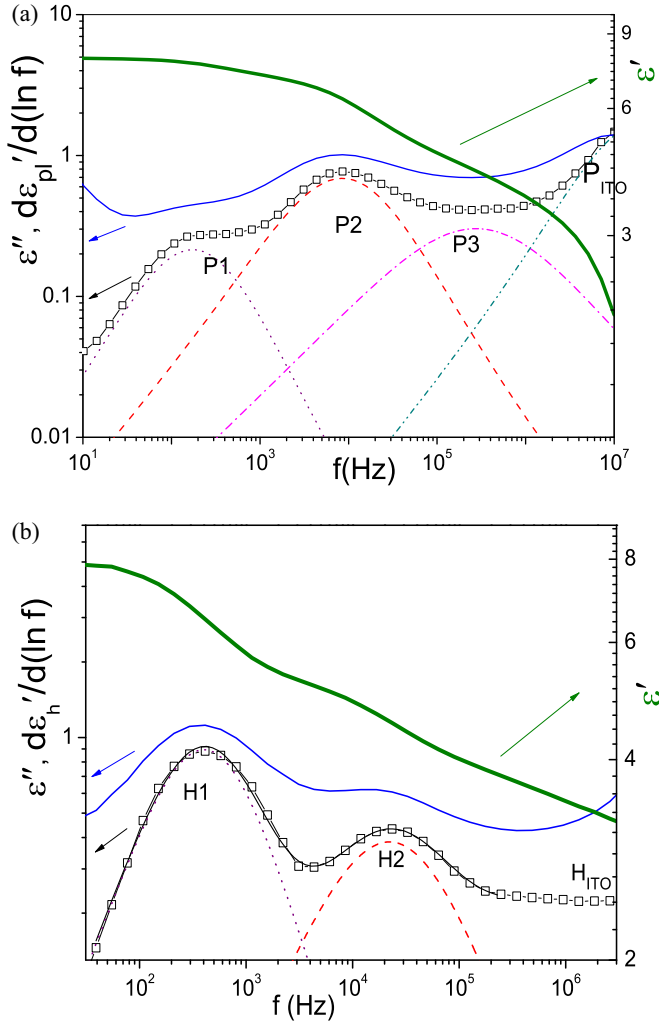


FIG. 5. (Color online) Frequency plots of the relative dielectric permittivity obtained from (a) planar cell at a reduced temperature ($T - T_{NI} = -22$ °C) and (b) homeotropic cell ($T - T_{NI} = -16$ °C): green (upper-thicker) line denotes ϵ' , blue (lower-thinner) line denotes ϵ'' , \square symbol represents $d\epsilon'/d(\ln f)$ [the derivative of ϵ' with respect to $(\ln f)$]. In (a) and (b), the dotted, dashed, dashed-dotted, and dashed-dashed-dotted lines are the deconvoluted components of $d\epsilon'/d(\ln f)$. P1, P2, P3, and P_{ITO} are the relaxation peaks for the planar cell given in (a); H1, H2, and H_{ITO} are the modes obtained in the homeotropic configuration shown in (b).

terms of the Maier and Meier (M-M) model given by Dunmur and Toriyama [18]. These sets of equations express relations between ϵ'_{\parallel} and ϵ'_{\perp} and the molecular parameters, such as the components of the dipole moment and the orientational order parameter. The principal permittivity components and the dielectric anisotropy in this model are explained from the overall dipole moment μ acting parallel and perpendicular to the molecular long axis [18],

$$\epsilon_{\parallel}(0) - n_{\parallel}^2 = \frac{NhF^2g_{\parallel}}{3\epsilon_0k_B T} [\mu_l^2(1 + 2S) + \mu_t^2(1 - S)], \quad (3)$$

$$\epsilon_{\perp}(0) - n_{\perp}^2 = \frac{NhF^2g_{\perp}}{3\epsilon_0k_B T} \left[\mu_l^2(1 - S) + \mu_t^2 \left(1 + \frac{1}{2}S \right) \right]. \quad (4)$$

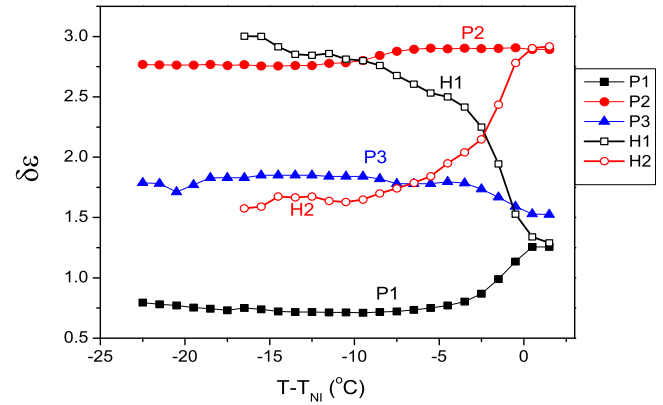


FIG. 6. (Color online) The dielectric strengths ($\delta\epsilon$) corresponding to the various relaxation processes P1, P2, and P3 (planar configuration) and H1 and H2 (homeotropic configuration) as a function of the reduced temperature. Peaks identified as: P1 and H1 correspond to the rotation around the short molecular axis of the rodlike molecules, P2 and H2 are due to rotation around the long molecular axis of the bent-core mesogen, and P3 is due to the rotation around the long molecular axis of the rodlike mesogen.

Here μ_l and μ_t are the longitudinal and transverse components of the molecular dipole moment with respect to the molecular long axis. $A = NhF^2/3\epsilon_0k_B$ is the scaling factor for each dipolar contribution to the dielectric relaxation strength. N is the number density of molecules, ϵ_0 is the permittivity of vacuum, T is the absolute temperature, F and h are the internal field factors for the reaction and the cavity fields, respectively. g_{\parallel} and g_{\perp} are the anisotropic Kirkwood correlation factors of the director parallel and perpendicular to the applied electric field, respectively. S is the orientational order parameter, $k_B T$ is the thermal energy, and k_B is the Boltzmann constant. It is worth mentioning that no macroscopic biaxiality was observed in the nematic phase of BR1 when investigated using the polarized IR technique [17]. Hence it may seem reasonable to apply the M-M model for explaining the dielectric results of BR1.

Using Eqs. (3) and (4), we calculated the internal field factors for the reaction field (F) and cavity field (h) at the

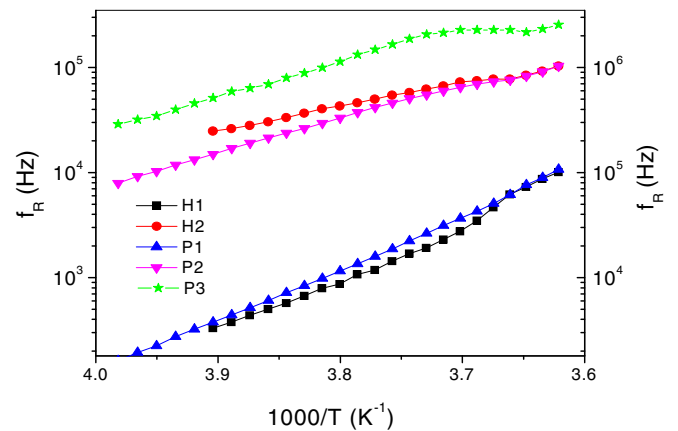


FIG. 7. (Color online) Relaxation frequency (f_R) for the various relaxation processes as a function of the reciprocal temperature (K^{-1}). The frequency scale on the right refers to the mode P3 only

transition temperature where $S \cong 0$ and the following values were found: $F = 1.42$ and $h = 1.44$. The number density was calculated to be $N = 0.43 \times 10^{27} \text{ m}^{-3}$ by assuming the material density to be 1100 kg/m^3 . Here the scaling factor A is found to be $3.35 \times 10^{60} \text{ KC}^{-2} \text{ m}^{-2}$.

According to M-M equations, μ_l and μ_t are the determining factors for the temperature dependencies of dielectric strength $\delta\epsilon$ and the dielectric anisotropy $\Delta\epsilon'$. The dielectric anisotropy in the nematic phase is given by the formula derived by Maier-Meier as follows [18]:

$$\Delta\epsilon' = \frac{NFH}{\epsilon_0} \left[\Delta\alpha - \frac{\mu^2 F (1 - 3 \cos^2 \beta)}{2kT} \right] S. \quad (5)$$

In Eq. (5), the anisotropy in the polarizability $\Delta\alpha$ is proportional to $(n_{\parallel}^2 - n_{\perp}^2)$, and β is the angle between the long molecular axis and the dipole moment. From Eq. (5) $\Delta\epsilon'$ can be negative, depending on $\Delta\alpha$ and the angle β . In liquid crystalline molecules, various conformations are possible due to the intramolecular degrees of freedom. As the temperature is lowered, conformations may change the angle between the effective dipole moment and the long molecular axis; this may affect the overall dielectric results in such systems. Recent studies on some bimesogens constituted of rodlike mesogens have revealed the influence of the conformational change in the dielectric results of such materials [19]. The changes arising from the orientation of one of the constituent mesogens due to the change in the conformational state of the flexible spacer causes a change in the magnitude and direction of the dipole moment with temperature. This results in a low frequency dielectric relaxation [19] in such systems. There is thus a possibility that conformational changes in BR1 may also be responsible for the observed low frequency relaxations. However, the bimesogenic molecule studied here is too large to show relaxation as a whole, and furthermore if that were the case the relaxation frequency would be much below 1 Hz. It is thus more likely that the dynamics of the constituent mesogens is fairly decoupled from each other and it is reasonable to consider separate contributions of each mesogen to the dielectric permittivity and adding a small contribution from the SiOSi electric dipole moment. In the low temperature range, an imperfect decoupling may have an impact on the correlation factors in Eqs. (3) and (4) where fitting of the experimental data to these equations is rather poor.

From Eqs. (3) and (4), one notes that the dielectric strength of each relaxation process is primarily dependent on the order parameter S . By comparing the temperature dependencies of $\delta\epsilon$ for the different relaxation processes in Fig. 6, it is quite evident that the dielectric strength of peaks P1 and H2 are proportional to $(1-S)/T$ and H1 and P3 are proportional to $(1+2S)/T$ and $(1+S/2)/T$, respectively. The temperature dependence of peak P2 looks rather unusual in the sense that it rises with temperature, but such behavior could arise from large anisotropic correlations of the components of the dipole moment. Solid lines in Fig. 8 show how the M-M model reproduces the experimental data for the homeotropic configuration. Blue and magenta lines show the temperature dependencies of H1 and H2 on the $(1+2S)$ and $(1-S)$ terms, respectively, of Eq. (3). Similarly, P1 and P3 showed $(1-S)$ and $(1+S/2)$ dependencies on temperature, respectively, for

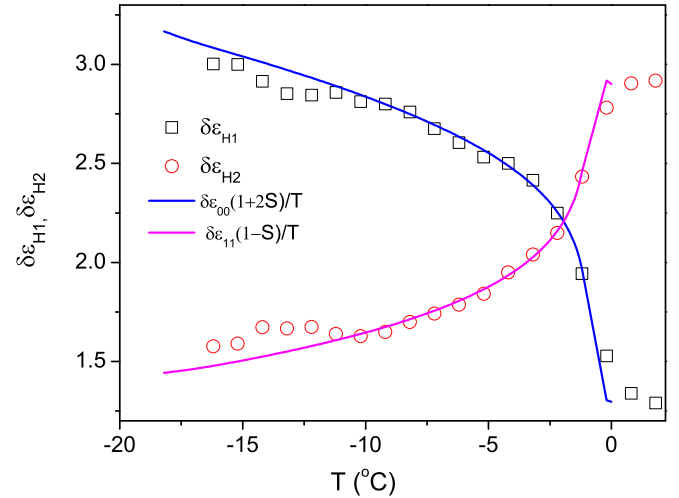


FIG. 8. (Color online) The dielectric strength corresponding to H1 (\square) and H2 (\circ) (red); fit of the data to the M-M model shown by the solid lines.

the fit of the corresponding dielectric strengths to Eq. (4) [Fig. 6, details of the fit not shown here]. By analyzing the fit of the M-M model to the dielectric strength data and the corresponding relaxation frequencies, a proper assignment can thus be made for each relaxation process.

Based on these results, we conclude that peaks P2 and H2 correspond to the relaxation of the transverse components of the BC mesogen, peaks H1, P1, and P3 are due to the RL mesogen. H1 and P1 correspond to the relaxations of the longitudinal component, whereas P3 is due to the relaxation of the transverse component. The highest frequency peaks H_{ITO} and P_{ITO} are presumably due to the ITO contributions. The dielectric strengths of peaks P1, P2, and P3 are found to be 1.25, 2.92, and 1.52, respectively, at temperatures just above the transition temperature. In addition to this, we estimated the dielectric strength of the relaxation of peak H0 ($\delta\epsilon = 0.95$), which is due to the relaxation of the longitudinal dipole component of the bent-core mesogen.

Apart from the scaling factor A , both the longitudinal (μ_l) and the transverse (μ_t) components of the molecular dipole moment can be obtained from the fitting of the dielectric strength data to the M-M equation. We calculated the square of the effective total dipole moment, from Eqs. (3) and (4), $\mu_{\text{eff}}^2 = [\epsilon(0) - n^2]T/A$, by assuming $S \cong 0$ at the phase transition) to be 61.8 D^2 , thus $\mu_{\text{eff}} = 7.86 \text{ D}$. The mesogens are linked by a flexible chain, and hence it is more likely that their reorientation is more or less independent from each other. For the case of independent reorientations we have four contributions to the dielectric permittivity, μ_{IBC} , μ_{tBC} , μ_{IRL} , and μ_{tRL} , related to the square of these dipole moments. The dipole moment of each component is calculated using its corresponding dielectric strength. These are found as follows: $\mu_{IBC} = 2.97 \text{ D}$, $\mu_{tBC} = 5.21 \text{ D}$, $\mu_{IRL} = 3.41 \text{ D}$, and $\mu_{tRL} = 3.76 \text{ D}$. It is interesting to note that these values are rather close to the simulated values of the dipole moments (see the caption of Fig. 1).

The order parameter S has been calculated from the homeotropically aligned sample (as it is less influenced by the

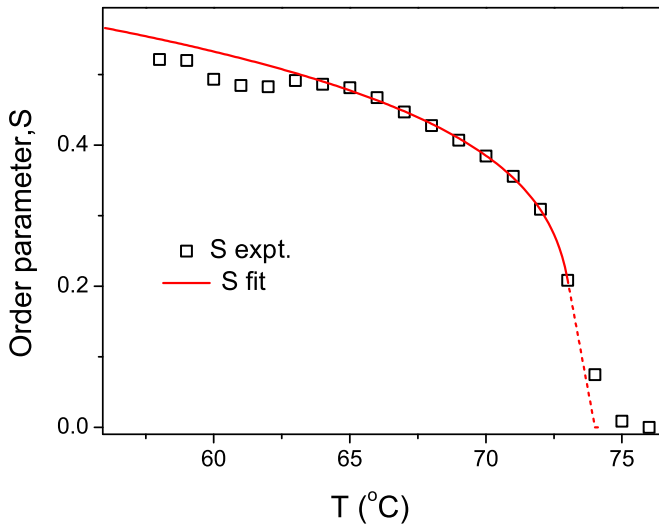


FIG. 9. (Color online) The order parameter as a function of temperature calculated from the experimental data for the homeotropic cell. The solid red line represents the fit of S to the power law $(1 - T/T_{NI})^\gamma$, γ is the critical exponent = 0.24. Note that S for the bent-core system studied here though typical is generally lower than for the calamitics.

surface boundaries) using the dielectric strengths corresponding to the H1 and H2 modes. For the homeotropic configuration we can use both terms in the parentheses of Eq. (3) and apply the same scaling factor A to the corresponding dielectric strength data in the temperature range below the isotropic to nematic transition to obtain S . Figure 8 shows the temperature behavior of each term. If we assume $g_{\parallel} = 1$, then the order parameter determined from H2 is slightly higher than that obtained from H1. In order to achieve self-consistency of the results, we allow g_{\parallel} to depart from unity ($g_{\parallel} \cong 1.05$, see Fig. 10). Figure 9 shows the resulting order parameter from experimental data and its fit by the power law $(1 - T/T_{NI})^\gamma$, where γ is the critical exponent ($\gamma = 0.24$). The solid lines in Fig. 8 show how the M-M model correctly reproduces the experimental data. The same S data can be used to reproduce experimental data for the planar alignment by allowing g_{\perp} to be different for the bent-core and rodlike mesogens. The determined correlation factors show relatively different temperature dependencies and are plotted in Fig. 10.

The theoretical evaluation of the anisotropic correlation factors requires a detailed microscopic model. A model proposed by de Jeu *et al.* [20] considers the clusters as smecticlike structures on the assumption that $S = 1$ so that the molecules are constrained to be either parallel or antiparallel to the director axis. For the smectic order, the average separation perpendicular to the layers (r_z) is likely to be greater than the in-plane separation (r_x), and this results in $g_{\parallel} < 1$, indicating antiparallel correlation with longitudinal dipoles. If $\langle r_x^2 \rangle < \langle r^2 \rangle / 3$, where $\langle r \rangle$ is defined as the average distance between two molecules, we get $g_{\perp} > 1$ favoring a parallel alignment of the polar axes [18].

From the experimental data obtained here for BR1, we find that the g_{\perp} factor for the rodlike mesogen is greater than 1, which is usual in the smectic order. This indicates

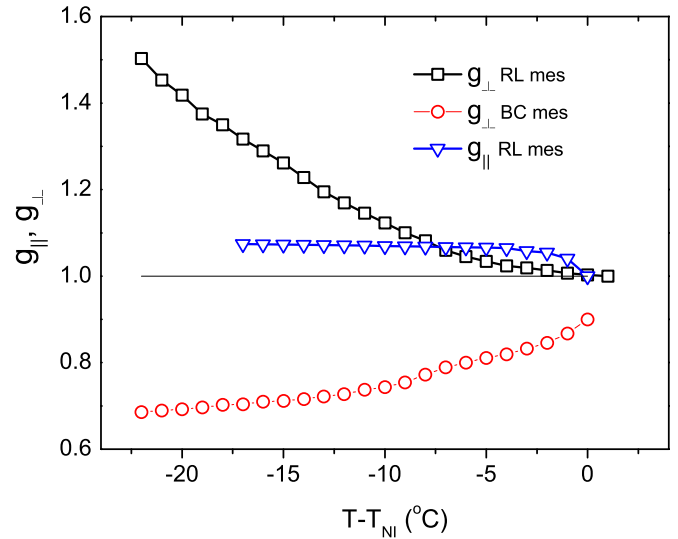


FIG. 10. (Color online) Temperature dependencies of the g factors. g_{\parallel} and g_{\perp} are the anisotropic Kirkwood correlation factors for the director parallel and perpendicular to the electric field, respectively.

parallel correlation of the transverse dipoles, which is seen to grow with decreasing temperature. On the contrary, the g_{\perp} factor for bent-core mesogen is below 1, which indicates rather antiparallel correlation of transverse dipoles, and this tendency of antiparallel association increases with lowering temperature.

We performed similar correlation studies for the three bent-core liquid crystals (C4, C7, and C9) with the same mesogenic core 4-cyanoresorcinol bisbenzoate as BR1 but with different terminal groups [12]. The temperature dependencies of permittivity were related to a change in the strong anisotropic correlations among the molecules. By using the experimental values obtained for g_{\perp} , we calculated the number of interacting molecules for a smecticlike order in the bent-core materials [12]. The average separation values perpendicular r_z and parallel r_x to the smectic layer were taken from the

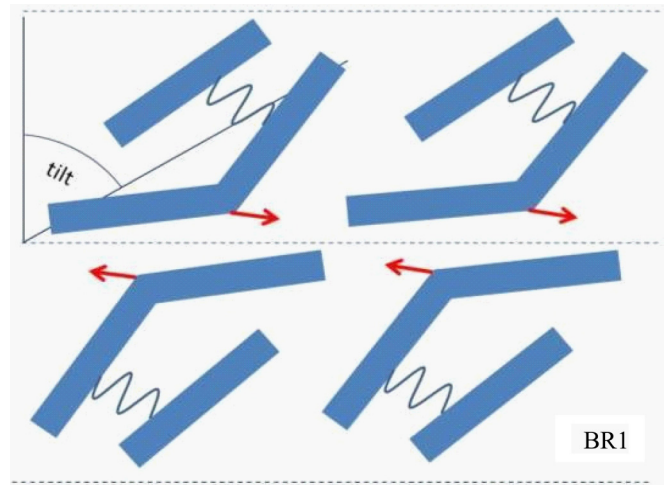


FIG. 11. (Color online) Possible arrangement of the mesogenic units in smectic layers. The system in the nematic phase has a local smecticlike structure.

small-angle x-ray scattering and wide-angle peak positions, respectively. We found that on increasing the chain length, the separation along the layer normally increases but the corresponding separation within the layer decreases. As a result g_{\perp} gradually increases and g_{\parallel} decreases. We also noted from Fig. 6 in Ref. [12] that the size of the cluster increases on reducing the temperature.

In the dimesogen studied here the introduction of the rodlike mesogenic core may also reinforce dipole-dipole interactions perhaps in a different manner, and it is therefore interesting to explore how the correlation factors g_{\perp} and g_{\parallel} behave differently with temperature. It is shown from the analysis of the dielectric modes of BR1 that the rodlike mesogenic core unit attached laterally to the bent-core mesogenic unit, composed of 4-cyanoresorcinol bisbenzoate, brings g_{\perp} below unity and increases g_{\parallel} . This results in a possible arrangement of molecules within the smecticlike clusters, wherein the dipoles interact in an antiparallel manner (note $r_z < r_x$) as illustrated by the model shown in Fig. 11. The tilt angle represents the tilt of the molecules in the SmC like clusters.

From the above discussion it follows that temperature dependence of g_{\perp} and g_{\parallel} , in general, can be explained by decreasing the average separation perpendicular to the layers (r_z) and at the same time increasing the average separation of the molecules in the in plane (r_x). Indeed, introduction of the laterally attached rodlike mesogenic core will increase the separation of the bent-core mesogenic units within the layers, but at the same time the effective layer thickness is significantly reduced ($d \sim 3.2$ nm from the small-angle scattering data [14]) with respect to single mesogen (3.8 nm) either due to a large tilt angle (50°) [14] and/or to a (inter) layer (inter) penetration, thus decreasing the separation length perpendicular to layers (r_z).

Figure 12 shows the x-ray diffraction patterns [Fig. 12(a)] of BR1 under a magnetic field and χ scans [Fig. 12(b)] over the diffused small-angle scattering (for $2\theta = 1.5^\circ - 4.0^\circ$) at temperatures of 65, 55, and 45 °C. It was observed that d , associated with the small-angle scattering, decreases as the temperature is reduced (d varies from 3.16 nm at $T = 65$ °C to 3.12 and 3.10 nm at $T = 55$ and 45 °C, respectively;

consistent with the thickness of a single layer), indicating that the layer thickness decreases with lowering temperature. This is consistent with the model that is based on the results of the dielectric studies. The average intermolecular distance for BR1, obtained from the wide-angle peak position, was found to remain unchanged with temperature. However, the result obtained for the wide-angle scattering is not very surprising as the position of this diffuse scattering is not only influenced by the packing of the aromatic cores, but also is influenced by the alkyl chains as well. Additionally, the silyl group too has a significant influence on the diffuse scattering. Due to the broad nature of this peak, it has not been possible to separate the individual contributions.

The proposed arrangement of the molecules within the clusters of the compound BR1, based on the dielectric results, indicate an antiparallel interaction of the dipoles between the neighboring layers. In order to investigate if there is an emergence of a local antiferroelectric structure, we performed polar switching measurements based on the current repolarization technique. These studies revealed that in the entire nematic range of BR1, no polar switching is observed under even relatively high triangular applied voltages (30 V/ μm , 5 μm planar cell; frequency range: 0.1–30 Hz). This confirms the nonpolar nature of the clusters.

IV. CONCLUSION

The dielectric behavior of BR1 as the first example of a bimesogen consisting of a bent-core unit combined with a laterally attached rodlike mesogenic core [14] is reported. For the bent-core mesogenic unit, a 4-cyanoresorcinol bisbenzoate core is chosen as this particular core unit is known to favor the formation of nematic phases [14]. The splitting of the small-angle scattering $\Delta\chi/2$ is found to be 50° , and this indicates that there is a significant tilt of molecules in the SmC like clusters. The material shows sign reversal of the dielectric anisotropy rather similar to that observed in dual frequency nematics composed of rodlike mesogens and this is caused primarily by the switching off of the contribution of the longitudinal component of the electric dipole moment for frequencies

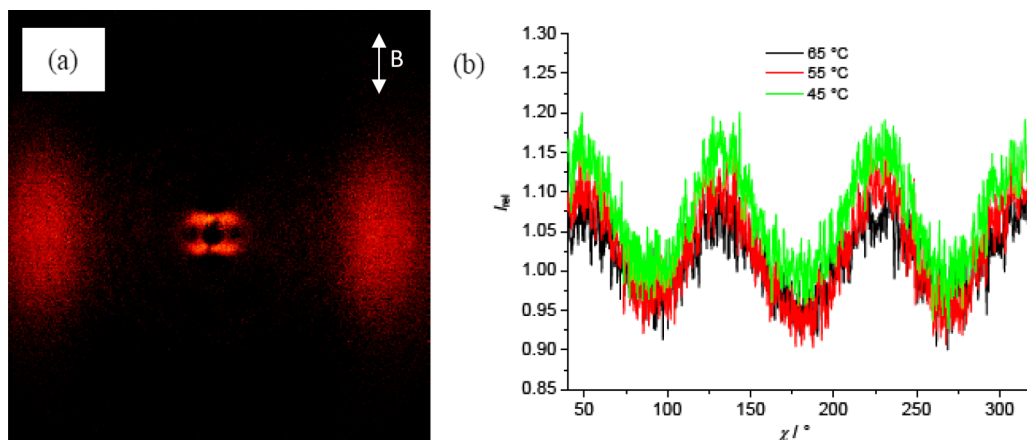


FIG. 12. (Color online) X-ray diffraction patterns of an oriented samples of compound BR1 under a magnetic field reproduced from [14] with permission from The Royal Society of Chemistry; the arrow denotes direction of the magnetic field; (a) The N_{cyBC} phase at 45 °C (shows the pattern after subtraction of the scattering in the isotropic liquid state $T = 80$ °C) and (b) χ scans over the diffused small-angle scattering (for $2\theta = 1.5^\circ - 4.0^\circ$) at 65, 55, and 45 °C, $I_{\text{rel}} = I(T)/I(80^\circ\text{C, Iso})$.

above its corresponding relaxation rate. However the sign reversal occurs at much lower frequencies in comparison to the calamitic and bent-core mesogens explored previously, and this is a consequence of the larger size of the bimesogen. On transition from the isotropic to the nematic phase of the bimesogen, the average permittivity is seen to decrease as temperature is lowered, and this indicates an onset of the antiparallel association of the dipoles, and this association increases as the temperature is lowered. Such an association is much more prominent in this bimesogen compared to other BCNs containing similar bisbenzoate cores [11(a),12]. The analysis of the dielectric loss spectra in terms of the M-M equations leads to a model where the dipoles in the neighboring layers interact in an antiparallel manner and the dipoles within the layers are parallel to each other. Results are supported by the x-ray scattering studies on this material. An apolar correlation between the clusters is revealed by the absence

of polar switching under an applied triangular wave, and this conclusion is valid even for relatively higher applied voltages.

ACKNOWLEDGMENTS

Collaboration between Dublin and Halle was funded by the EU FP7 BIND Project 2008-12 (Grant No. 216025). One of the authors (R.B.) thanks the Irish Research Council for support through a research studentship, and J.K.V. and A.K. thank the Science Foundation of Ireland for support through a Walton Visiting Professorship to A.K. The authors (K.M. and A.K.) thank the National Science Centre for Grant No. DEC 2011/03/B/ST3/03369. M. Nagaraj is thanked for making preliminary alignment measurements. The authors also thank Professor J. M. D. Coey and Dr. M. Venkatesan for allowing use of the facilities of a large magnet in their laboratory.

-
- [1] M. Tokita, K. Osada, and J. Watanabe, *Liq. Cryst.* **24**, 477 (1998); G. Ungar, V. Percec, and M. Zuber, *Macromolecules* **25**, 75 (1992); A. Abe, H. Furuya, Z. Zhou, T. Hiejima, and Y. Kobayashi, *Adv. Polym. Sci.* **181**, 121 (2005).
- [2] C. T. Imrie and P. A. Henderson, *Chem. Soc. Rev.* **36**, 2096 (2007).
- [3] (a) G. Dantlgraber, S. Diele, and C. Tschierske, *Chem. Commun.* **23**, 2768 (2002); (b) B. Kosata, G.-M. Tamba, U. Baumeister, K. Pelz, S. Diele, G. Pelzl, G. Galli, S. Samaritani, E. V. Agina, N. I. Boiko, V. P. Shibaev, and W. Weissflog, *Chem. Mater.* **18**, 691 (2006).
- [4] (a) M. G. Tamba, B. Kosata, K. Pelz, S. Diele, G. Pelzl, Z. Vakhovskaya, H. Kresse, and W. Weissflog, *Soft Matter* **2**, 60 (2006); (b) C. V. Yelamaggad, S. K. Prasad, G. G. Nair, I. S. Sashikala, D. S. Shanker Rao, C. V. Lobo, and S. Chandrasekhar, *Angew. Chem., Int. Ed.* **43**, 3429 (2004); (c) G. Shanker, M. Prehm, and C. Tschierske, *Beilstein J. Org. Chem.* **8**, 472 (2012).
- [5] C. T. Imrie, P. A. Henderson and G. Y. Yeap, *Liq. Cryst.* **36**, 755 (2009).
- [6] C. T. Imrie and G. R. Luckhurst, in *Handbook of Liquid Crystals*, edited by D. Demus, J. W. Goodby, G. W. Gray, H. W. Speiss, and V. Vill (Wiley-VCH, Weinheim, 1998), pp. 801.
- [7] R. W. Date and D. W. Bruce, *J. Am. Chem. Soc.* **125**, 9012 (2003); P. H. Kouwer and G. H. Mehl, *ibid.* **125**, 11172 (2003); D. Apreutesei and G. H. Mehl, *Chem. Commun.* **6**, 609 (2006).
- [8] G. S. Attard, R. W. Date, C. T. Imrie, G. R. Luckhurst, S. J. Roskilly, J. M. Seddon, and L. Taylor, *Liq. Cryst.* **16**, 529 (1994); J. W. Goodby, I. M. Saez, S. J. Cowling, J. S. Gasowska, R. A. MacDonald, S. Sia, P. Watson, K. J. Toyne, M. Hird, R. A. Lewis, S.-E. Lee, and V. Vaschenko, *ibid.* **36**, 567 (2009).
- [9] C. Meyer, G. R. Luckhurst, and I. Dozov, *Phys. Rev. Lett.* **111**, 067801 (2013); V. Borshch, Y.-K. Kim, J. Xiang, M. Gao, A. Jáklí, V. P. Panov, J. K. Vij, C. T. Imrie, M. G. Tamba, G. H. Mehl, and O. D. Lavrentovich, *Nat. Commun.* **4**, 2635 (2013); D. Chen, J. H. Porada, J. B. Hooper, A. Klitnick, Y. Shen, M. R. Tuchband, E. Korblova, D. Bedrov, D. M. Walba, M. A. Glaser, J. E. MacLennan, and N. A. Clark, *Proc. Natl. Acad. Sci. USA* **110**, 15931 (2013); R. Balachandran, V. P. Panov, Y. P. Panarin, J. K. Vij, M. G. Tamba, G. H. Mehl, and J. K. Song, *J. Mater. Chem. C*, **2**, 8179 (2014); V. P. Panov, R. Balachandran, M. Nagaraj, J. K. Vij, M. G. Tamba, A. Kohlmeier, and G. H. Mehl, *Appl. Phys. Lett.* **99**, 261903 (2011); V. P. Panov, R. Balachandran, J. K. Vij, M. G. Tamba, A. Kohlmeier, and G. H. Mehl, *ibid.* **101**, 234106 (2012); V. P. Panov, M. Nagaraj, J. K. Vij, Y. P. Panarin, A. Kohlmeier, M. G. Tamba, R. A. Lewis, and G. H. Mehl, *Phys. Rev. Lett.* **105**, 167801 (2010).
- [10] E. P. Raynes and I. Shanks, *Electron Lett.* **10**, 114 (1974); M. Schadt, *Annu. Rev. Mater. Sci.* **27**, 305 (1997).
- [11] (a) Y. Jang, V. P. Panov, C. Keith, C. Tschierske, and J. K. Vij, *Appl. Phys. Lett.* **97**, 152903 (2010); (b) J. K. Song, U. Manna, A. Fukuda, and J. K. Vij, *ibid.* **91**, 042907 (2007).
- [12] Y. Jang, V. P. Panov, A. Kocot, A. Lehmann, C. Tschierske, and J. K. Vij, *Phys. Rev. E* **84**, 060701(R) (2011).
- [13] S. A. Jewell and J. R. Sambles, *Appl. Phys. Lett.* **87**, 021106 (2005).
- [14] G. Shanker, M. Prehm and C. Tschierske, *J. Mater. Chem.* **22**, 168 (2012).
- [15] Y. P. Panarin, H. Xu, S. T. Mac Lughadha, and J. K. Vij, *Jpn J. Appl. Phys., Part 1* **33**, 2648 (1994).
- [16] K. Merkel, A. Kocot, J. K. Vij, G. H. Mehl, and T. Meyer, *Phys. Rev. E* **73**, 051702 (2006); L. Tajber, A. Kocot, J. K. Vij, K. Merkel, J. Zaleswska-Rejdak, G. H. Mehl, R. Elsässer, J. W. Goodby, and M. Veith, *Macromolecules* **35**, 8601 (2002).
- [17] K. Merkel, A. Kocot, J. K. Vij, G. H. Mehl, and T. Meyer, *J. Chem. Phys.* **121**, 5012 (2004); A. Kocot, R. Wrzalik, and J. K. Vij, *Liq. Cryst.* **21**, 147 (1996).
- [18] D. Dunmur and K. Toriyama, in *Handbook of Liquid Crystals*, edited D. Demus, J. Goodby, G. W. Gray, H. W. Speiss, and V. Vill (Wiley-VCH, Weinheim, 1998), Vol. 1, p. 231.
- [19] M. Stocchero, A. Ferrarini, G. J. Moro, D. A. Dunmur, and G. R. Luckhurst, *J. Chem. Phys.* **121**, 8079 (2004).
- [20] W. H. de Jeu, W. J. A. Goossens, and P. Bordewijk, *J. Chem. Phys.* **61**, 1985 (1974).